Heroin Cue-Evoked Astrocytic Structural Plasticity at Nucleus Accumbens Synapses Inhibits Heroin Seeking

Anna Kruyer[1,*], **Michael D. Scofield**[1,2], **Daniel Wood**[1], **Kathryn J. Reissner**[3], **Peter W. Kalivas**[1,*]

[1]Department of Neurosciences, Medical University of South Carolina, Charleston, SC, USA.

[2]Department of Anesthesia and Perioperative Medicine, Medical University of South Carolina, Charleston, SC, USA.

[3]Department of Psychology and Neuroscience, University of North Carolina at Chapel Hill, Chapel Hill, NC, USA.

Abstract

BACKGROUND—Opioid addiction is a critical medical and social problem characterized by vulnerability to relapse. Glutamatergic synapses in the nucleus accumbens regulate the motivation to relapse to opioid use and down-regulation of glutamate transporters on astroglial processes adjacent to accumbens synapses contributes to heroin seeking induced by cues. However, it is not known how astroglial processes themselves respond to heroin cues or if changes in astroglial morphology are necessary for heroin seeking.

METHODS—Male Sprague-Dawley rats (n=62) were trained to self-administer heroin or sucrose and were reinstated by heroin- or sucrose-conditioned cues. Astroglial proximity to accumbens synapses was estimated using a confocal-based strategy and the association between digitally isolated astroglia and the presynaptic marker Synapsin I was quantified. To determine the functional consequence of astroglial morphological plasticity on cued heroin seeking, a morpholino antisense strategy was used to knock down expression of the actin binding protein ezrin, which is expressed almost exclusively in peripheral astrocyte processes in the adult rat brain.

RESULTS—After heroin extinction, there was an enduring reduction in synaptic proximity by astroglia. Synaptic proximity was restored during 15 min of cued heroin seeking, but returned to extinction levels by 120 min. Extinction from sucrose self-administration and reinstated sucrose-seeking induced no changes in astroglial synaptic association. Ezrin knockdown reduced astroglial association with synapses and potentiated cued heroin seeking.

---

*Correspondence should be addressed to A.K. (173 Ashley Ave, MSC510, Charleston, SC, 29425; 843-876-2246, kruyer@musc.edu) or P.W.K. (173 Ashley Ave, MSC510, Charleston, SC 29425; 843-876-2340, kalivasp@musc.edu).

CONCLUSIONS—Cue-induced heroin seeking transiently increased synaptic proximity of accumbens astrocytes. Surprisingly, the re-association of astroglia with synapses was compensatory, and preventing cue-induced morphological plasticity in astrocytes potentiated heroin seeking.

Keywords

astrocyte; addiction; heroin; nucleus accumbens; synapse; self-administration

INTRODUCTION

Astrocytes are the most abundant glial cell type in the brain. Long considered support cells for maintaining neuronal metabolic homeostasis, a growing literature demonstrates that astrocytes directly regulate neuronal activity, in part through peripheral processes that contact up to 90% of synapses in some brain regions (1, 2). The peripheral processes of astrocytes are irregular protrusions lacking glial fibrillary acidic protein (GFAP)-containing filaments, microtubules and organelles (3) that *in vitro* undergo structural plasticity in response to excitatory synaptic activity (4). Astrocytes also regulate levels of extracellular glutamate via uptake and release, and promote the stability of dendritic spines (5). Their capacity to simultaneously interact with tens of thousands of synapses physically situates astrocytes to coordinate neurocircuit dynamics, and play a role in circuit pathologies thought to underlie neuropsychiatric disorders (6).

Astrocytes gather information from neurons via the spillover of synaptically released transmitters, and spillover of glutamate in the core subcompartment of the nucleus accumbens (NAcore) is necessary for drug-, but not sucrose-associated cues to reinstate seeking in rodent models of cue-induced relapse (7, 8). While the shell subcompartment of the NA is also involved in the processing of drug-reward contingencies and contributes to drug seeking in response to drug-associated contexts and priming injections, we focus here on the NAcore due to its central role in producing seeking behavior in response to drug-associated cues (8). Glutamate spillover in the NAcore arises because repeated administration of all addictive drugs examined to date, including cocaine, heroin, nicotine, and alcohol, reduces the expression and/or function of the glial glutamate transporter (GLT-1) (7, 8), which is preferentially expressed on astroglial processes (9, 10). Moreover, computational modeling of astroglial perisynaptic processes demonstrate that astroglial insulation along 50% of the synaptic perimeter doubles glutamate concentrations within the synaptic cleft and produces a 2–4-fold decrease in extrasynaptic glutamate (11). Thus, through morphological plasticity, astrocyte cytoarchitecture regulates the balance between synaptic and extrasynaptic glutamate (12). Although drug-induced reductions in NAcore GLT-1 are linked to relapse in animal models of addiction, the capacity of the astroglial membrane to undergo rapid morphological changes *in vitro* indicates that changes in astrocyte morphology and synaptic proximity may also impact extracellular glutamate levels *in vivo* and regulate the capacity of drug cues to initiate seeking. Here we demonstrate that the *in vivo* association of astrocytes with the presynaptic marker Synapsin I (13) in the NAcore is constitutively reduced after heroin use, and is transiently restored by cues that predict heroin delivery. To determine the functional consequence of the morphological

plasticity we observed in NAcore astrocytes in response to heroin cues, we took advantage of the fact that ezrin is an actin-binding protein expressed primarily by astrocytes in the adult rat brain that links actin with the astroglial membrane in peripheral processes (14, 15). We show that knockdown of ezrin reduced astroglial association with the synapse and elevated cued heroin seeking, suggesting an important role for transient astroglial plasticity in attenuation of drug seeking.

METHODS AND MATERIALS

Self-Administration

Male Sprague Dawley rats (200–250 g) were purchased from Charles River and housed individually in a temperature-controlled environment on a 12-hour reverse light cycle. Following approximately 1 week of acclimation, animals undergoing heroin self-administration or receiving yoked saline infusions were anesthetized with ketamine/xylazine (100 mg/kg and 7 mg/kg, IM) and fitted with intra-jugular catheters. Ketorolac (0.3 mg/kg, IM) was administered post-operatively as an analgesic and taurolidine-citrate catheter lock solution (0.05 mL, Access Technologies) was administered IV through the catheter beginning 48h after surgery and daily thereafter to maintain patency. Heroin or sucrose self-administering rats and yoked controls were maintained on 25g chow/d during the self-administration phase of operant training and received chow *ad libitum* thereafter. Animals were trained to self-administer sucrose (PO) or heroin (IV) during 3h sessions for 10 consecutive days, during which time presses on an active lever were paired with light and tone cues and either infusion of heroin (100 μg/infusion on d1–2, 50 μg/infusion on d3–4, 25 μg/infusion on all subsequent days) or delivery of a sucrose pellet (45 mg, Bio-Serv). The dosing strategy during heroin self-administration ensures that animals acquire self-administration and lever discrimination early during operant training (d1–2) and serves to elevate lever pressing above baseline after acquisition of operant responding (d5–10). Yoked controls received light and tone cues when a paired rat received sucrose or heroin. Those yoked to heroin self-administering animals also received passive infusions of saline. Following self-administration, animals underwent 10–14d of extinction training (3h/d) during which time presses on the active lever had no consequence. Extinguished animals and yoked controls were sacrificed 24h after the last extinction session. Reinstated animals were placed in the operant chamber a final time and light/tone pairings were restored to the active lever, but animals received no reward. The session continued for 15 or 120 minutes before sacrifice. Animals with >10 active lever presses within the first 15 minutes of reinstatement trials were considered to reinstate and were included in subsequent analyses. All animals were anesthetized with pentobarbital (1–2mg, IV) and perfused transcardially with 60mL 0.1M phosphate buffer and 120mL 4% PFA. Brains were removed, incubated overnight in 4% PFA and sliced at 100 μm on a vibrating-blade microtome (Thermo Scientific). Tissue was collected into PBS with 0.05% sodium azide and stored at 4C until use.

Viral Labeling and Immunohistochemistry

Immediately following catheter implantation or 5d before the start of sucrose self-administration, animals received microinjections (1.0 μL/hemisphere, 0.15 μL/minute, 5 min diffusion) of a virus driving expression of membrane-targeted mCherry under control of the

GFAP promoter (AAV5-GFAP-hM3dq-mCherry, University of Zurich). mCherry was tagged to hM3dq which is a membrane targeted Gq-coupled designer receptor exclusively activated by designer drugs (DREADD). For the experiments in this report the DREADD was used only for membrane targeting of mCherry, and was not activated. The virus was injected into the nucleus accumbens core (+1.5mm AP, ± 1.8mm ML, −7.0mm DV) with 26-gauge injectors (Plastics One Inc.). Virus incubation occurred over the course of self-administration and extinction training (~4 wks). Following perfusion and sectioning, slices containing the nucleus accumbens core were permeabilized in 1XPBS with 2% Triton X-100 for 1h at room temperature before blocking in 1XPBS with 0.2% Triton X-100 (PBST) with 2% normal goat serum (block). Primary antibodies against Synapsin I (Abcam Cat# ab64581, RRID:AB_1281135; 1:1000), ezrin (Cell Signaling Technology Cat#3145, RRID:AB_2100309; 1:1000), radixin (Abcam Cat# ab52495, RRID:AB_882259), moesin (Abcam Cat# ab52495, RRID:AB_881245), or phosphor-ezrin(Thr567)/radixin(Thr564)/moesin(Thr558) (Cell Signaling Technology Cat#3726, RRID:AB_10560513; 1:1000) were diluted in block and sections were incubated for 2d at 4°C with gentle agitation. Virally expressed mCherry was visualized without antibody amplification. Slices were washed in PBST before incubation in fluorescent secondary antibodies (AlexaFluor, 1:1000) in PBST for 1d at RT. After washing in PBST, tissue was mounted onto glass slides and coverslipped using ProLong Gold Antifade Reagent (Thermo Fisher Scientific).

Imaging Acquisition and Analysis

Z-stacks were acquired using a Leica SP5 laser-scanning confocal microscope equipped with argon, krypton and helium/neon beams. All images were acquired using a 63X oil immersion objective lens with 1.7X digital zoom, 1024×1024 frame size, 12-bit image resolution, 4-frame averaging and 1-μm step size. Astrocytes were acquired if and only if the entire cellular volume could be imaged within the tissue section and the boundaries of the cell were not overlapping with nearby labeled cells. Acquired stacks were iteratively deconvolved 10 times (AutoQuant). Digital analysis of mCherry signal intensity relative to proximal background intensity was used to build a digital model of the astroglial volume (Bitplane Imaris). Colocalization (astrocyte with Synapsin I, astrocyte with ezrin, astrocyte surface with p-ERM) was determined based on thresholded signal intensity in each channel. Voxels containing fluorescence signal intensity greater than noise for each channel, determined empirically using a two-dimensional scatter plot within the colocalization module, were used to build a colocalization channel and acquire volume, puncta number, and puncta volume parameters. Total Synapsin I, radixin and moesin immunoreactivity was determined based on thresholded signal intensity and normalized to the volume of the frame from which it was acquired. Surface expression was determined by excluding colocalized signal >200nm from the astrocyte membrane. All imaging and image analyses were conducted blind to animal treatment.

Ezrin Knockdown

Animals undergoing treatment with antisense or control morpholino received bilateral cannulae placed just above the NAcore immediately following catheter surgery. Guide cannulae were used for viral labeling prior to operant training and for application of ezrin antisense or control oligos during extinction training. Beginning on day 7 of extinction for 3

consecutive days, animals received bilateral infusions (1 μL, 0.15 μL/min, 5 min diffusion) of an antisense oligomer targeted to ezrin (GCGCTCCGCAGGTTTCACTTCGTGA, 50 μM) or a nonspecific control sequence (Gene Tools, Inc.). After 3 additional days of extinction training, animals were reinstated using cues and their behavior was monitored.

Experimental Design and Statistical Analysis

All numerical data were analyzed using GraphPad Prism 7 and are presented as scatter plots with the median indicated for each group. For each measure, data were analyzed using D'Agostino-Pearson omnibus normality test followed by Kruskal-Wallis nonparametric test, because in all cases at least one treatment group was found to be not normally distributed (see Supplemental Table 1). Additionally, cumulative distribution plots of yoked saline measurements were used to identify 3 equal subpopulations of astroglia for each measure. Population criteria were applied across all treatment groups and differences between treatment groups in astroglial subpopulations were determined using Chi^2. In all cases, p-values <0.05 were considered significant.

RESULTS

Heroin and sucrose self-administration, extinction and cued seeking

Prior to beginning heroin self-administration, NAcore astroglia were transfected with a membrane reporter (AAV5-GFAP-hM3dq-mCherry) to allow confocal imaging, digitization and quantification of cell morphology (Figure 1A). Since all animals in this study received virus infusions and all imaged astrocytes expressed the membrane tag, any potential alterations in Ca^{2+} flux or GPCR signaling induced by the DREADD attached to mCherry would be expected to be equivalent across groups. Rats were trained to self-administer heroin or were yoked saline controls (Figure 1B,C; Supplemental Figure S1 for inactive lever presses). The heroin-trained rats were divided into three treatment groups such that all groups had the same total heroin intake (Figure 1C, inset). Lever pressing was extinguished over 10–14 days of training where heroin and cues were not delivered in response to active lever presses (Figure 1B,C). Heroin seeking was then induced in the absence of heroin delivery by restoring the light/tone cue previously associated with heroin infusion, and NAcore tissue slices were obtained 15 or 120 min after initiating cued heroin seeking (Figure 1B). Heroin cues reinstated active lever pressing relative to extinction levels of pressing after either 15 or 120 min, and the peak response occurred during the first 45 min of drug seeking (Figure 1D). A separate group of rats was trained to self-administer sucrose pellets using the same extinction and cue-induced reinstatement protocol as for heroin (Figure S2). Extinguished and reinstated rats were matched for average daily sucrose delivery (Figure S2A, inset), and rats reinstated to a similar level relative to cued heroin seeking in response to sucrose-paired cues (Figure S2B).

Astrocyte labeling and morphology

Astrocytes in the NAcore that were fully transfected with the mCherry membrane reporter were imaged and rendered using Imaris software (Figures 2 and S3). The digitally isolated and rendered astrocytes revealed a highly convoluted and irregular membrane surface, a morphological characteristic easily seen in a single z-plane obtained near the center of the

cell (Figure 2D–E, Figure S3). Astroglia are estimated to contact 20,000–160,000 individual synapses (16), but it is unknown to what extent astroglial interactions with synapses undergo plasticity in the adult brain. To estimate synaptic proximity by astroglia, tissue was double-labeled for the presynaptic marker Synapsin I (Figure 2A). Co-registration of immunoreactive Synapsin I puncta with the astroglial surface was digitally isolated and quantified to estimate the near-adjacency of astroglial membrane with NAcore Synapsin I (Figure 2B). This approach was developed because the diameter of fine astroglial processes (50–200 nm (17)) is below the limit of resolution for confocal microscopy (~250 nm (18)). In the striatum, distance of peripheral astroglial processes from excitatory synapses ranges between 10–400 nm, with 53% of synapses having astroglial coverage at a distance of <10nm (19). Thus, in the present report we operationally define near-adjacency as Synapsin I puncta co-registered with the astroglial membrane reporter by being within the 250 nm limit of image resolution (Figure 2E).

Examining a single plane from the z-stack near the middle of the astroglial volume showed that the astroglial surface extended throughout the astrocyte, and the presence of co-registered Synapsin I revealed abundant points of contact near the geometric center of the cell volume (Figure 2E, Figure S3). Total Synapsin I labeling between treatment groups was not different (Figure S4A), indicating that the changes described next in the heroin-trained rats arose from alterations in astroglial morphology, not Synapsin I density.

Heroin-associated cues restore synaptic proximity of NAcore astrocytes

Co-registration of the astroglial membrane with Synapsin I in the NAcore was reduced after extinction from heroin compared with yoked saline rats (Figure 2F), akin to our previous report in rats extinguished from cocaine self-administration (20). However, after 15 min of cue-induced heroin seeking, we observed rapid, transient re-association of astrocytic processes with Synapsin I that returned to extinction levels by 120 min after initiating cued reinstatement (Figure 2F, left panel). In accord with previous reports (6, 20), astroglial volume ranged from 5,000–50,000 μm^3 across all experimental groups (Figure S5). Because astroglial volume was reduced in rats reinstated for 15 min, data were analyzed with (Figure 2F) and without (Figure S4B) normalizing synaptic coverage to total astroglial volume. In both comparisons the 15 min reinstated group showed increased astroglia-Synapsin I proximity compared to extinguished rats.

Values for astroglia-Synapsin I proximity were not normally distributed in control rats (Table S1). Accordingly, we more closely examined the distribution of astroglia-synaptic proximity using cumulative frequency plots (Figure 2F–H, middle panel) that showed differences between treatment groups, and nonlinear breaks in the distribution curves supported possible subpopulations. Thus, data were divided into three subpopulations according to the values producing three equal populations in control rats (Figure 2F–H right; i.e. top, middle and bottom thirds). A Chi^2 analysis revealed that compared to saline rats, the extinguished group had nearly complete elimination of the astroglial subgroup containing the most astroglia-Synapsin I co-registration (Figure 2F, right). However, this subclass transiently returned after 15 min of cued reinstatement. In contrast to heroin-trained rats, rats

extinguished from sucrose self-administration or reinstated to sucrose-associated cues showed no alterations in astroglia-Synapsin I proximity (Figure S4C).

Cued astroglia-Synapsin I co-registration results from larger regions of overlap, not increased number of contacts

We next examined whether the transient plasticity in astroglia-Synapsin I proximity occurred because there were more Synapsin I puncta in contact with the astroglial membrane or the volume over overlapping regions had increased. Surprisingly, the number of puncta indicating near-adjacency between the astroglial membrane and Synapsin I did not change during 15 min of reinstated seeking (Figure 2G). Accordingly, the subgroup of astroglia that demonstrated the highest number of near-adjacent regions was eliminated in all heroin-extinguished rats regardless of whether or not they underwent cued reinstatement (Figure 2G, right). In contrast, the volume of astroglia-Synapsin I puncta showed dynamic changes after extinction and reinstatement (Figure 2H). Thus, the increased astroglia-Synapsin I proximity after 15 min of cued reinstatement observed in Figure 2F, arose from larger, but not more co-registered puncta after 15 min of cued reinstatement, and may indicate an increase in proximity of existing contacts (those <250 nm), rather than an increase in discrete points of contact between the astroglial membrane and Synapsin I.

Ezrin knockdown inhibits astroglia-Synapsin I re-association and augments cued seeking

To examine the molecular underpinnings and functional relevance of the cue-induced astroglial morphological plasticity we observed, we examined the Ezrin/Radixin/Moesin (ERM) family member protein ezrin and phosphorylated-ERM proteins (p-ERM). Ezrin and the other ERM proteins link the actin cytoskeleton with the astroglial membrane, allowing membrane protrusion and motility (21). In contrast with more widely distributed radixin and moesin, immuno-electron microscopy studies show that ezrin is highly selective for peripheral astroglial processes in the adult rat brain (14), with some evidence for expression in ependymal cells (22, 23). Ezrin is also expressed in microglia and neurons during early postnatal development (24). When phosphorylated, ezrin and other ERM proteins link actin to the membrane of astroglial processes, thereby enabling membrane protrusion (25). Immunohistochemical analysis for p-ERM and non-phosphorylated ezrin showed reduced p-ERM in heroin-extinguished rats, and restoration to control levels during 15-min of cued heroin reinstatement (Figure 3B). Importantly, total ezrin expression was equivalent across all treatment groups (Figure S7). The changes in ERM phosphorylation after extinction and 15 min of reinstatement were consistent with the observed changes in astroglia-Synapsin I association (Figure 2). Since ezrin exhibits the greatest selectivity for astroglial processes relative to radixin, moesin or other actin binding proteins (14), we examined ezrin knockdown as a strategy to impair the synaptic re-association by astrocytes during 15-minutes of cue exposure. Thus, another set of rats were trained to self-administer heroin and on d7 of extinction training, received bilateral infusions of an ezrin-targeted antisense oligomer in the NAcore for 3 consecutive days followed by 3 additional days of extinction training (Figure 3F). This timeline was selected because previous work demonstrated reduced protein expression 4d following the last of 3 consecutive days of morpholino infusion (26). Animals receiving ezrin and control sequences exhibited no differences in overall heroin intake during self-administration or active lever pressing during the last 2 days

of extinction training (Figure S8A,B). Compared to a standard control oligo, ezrin antisense markedly reduced ezrin protein detected by immunohistochemistry (Figure 3C,D), but did not alter radixin or moesin levels (Figure S9). The ezrin-targeted morpholino also reduced astroglia-Synapsin I association compared to control treatment by approximately the same percentage as extinction training (compare Figure 2F with 3E). Therefore, ezrin knock-down by morpholino was used to impair the astrocyte-synapse re-association induced by heroin cue exposure. When reinstated to heroin-associated cues, rats sustaining NAcore ezrin knockdown demonstrated greater active lever presses compared to control animals (Figure 3G), indicating a compensatory effect of the cue-induced astroglia-Synapsin I re-association. There was no alteration by ezrin knockdown on inactive lever presses (Figure S8C).

DISCUSSION

We used a confocal-based strategy to demonstrate that rats extinguished from heroin self-administration have reduced astroglial proximity to the synaptic marker Synapsin I in the NAcore. Although our work does not address the necessity of extinction training for this process, withdrawal appears necessary for retraction of astroglial processes from the synapse, since retraction was not observed 24 h after discontinuing cocaine self-administration (27). Surprisingly, the constitutive reduction in synaptic proximity was reversed after 15 min of cued heroin seeking. This reversal was transient and returned to extinction levels by the end of the 120 min reinstatement session, when active lever pressing had returned to the extinction baseline. The constitutive and cued transient changes in astroglia-Synapsin I proximity were not recapitulated in the NAcore of rats extinguished from sucrose self-administration and reinstated for 15 min using sucrose-associated cues. These data reveal remarkable rapid and transient astroglial morphological plasticity in response to cues that signal heroin availability, and support the emerging conceptualization that astrocytes partner with canonical pre- and postsynaptic elements to regulate synaptic transmission and homeostasis (28–31). Importantly, the lack of astroglial plasticity in response to cues signaling sucrose availability indicate that the observed astroglial plasticity may be a process that countermands the excessive motivation to relapse experienced by opioid users.

Astroglial plasticity is both pathogenic and compensatory

Synaptic spillover of glutamate during drug seeking is well documented using *in vivo* microdialysis or glutamate biosensors (8), as well as *in vitro* by measuring the effect of electrically stimulated glutamate release on the time constant of NMDA current decay (32). Spillover is thought to result from the fact that repeated treatment with most addictive drugs, including opioids, down-regulates the astroglial glutamate transporter GLT-1. However, the constitutive reduction in astroglial proximity to Synapsin I after cocaine (20) and heroin self-administration may also contribute to the capacity of drug cues to promote synaptic spillover in the NAcore. For example, the decreased astroglia-synapse proximity associated with heroin extinction would be expected to reduce the diffusion barrier through decreased synaptic insulation (11, 33) and proximity of the already reduced levels of GLT-1 on processes near glutamatergic synapses (34). Indeed, the lack of glutamate spillover during cue-induced reinstatement of sucrose seeking likely arises because repeated sucrose use does

not down-regulate GLT-1 (8) or produce changes in astroglia-Synapsin I proximity (Figure S4C).

In contrast to the constitutive reduction in astroglia-Synapsin I proximity after heroin withdrawal, the cue-induced restoration of proximity appeared to be compensatory. Thus, heroin cueinduced transient increases in synaptic proximity by astrocytes may compartmentalize glutamate spillover pre-synaptically, promoting the activation of release-regulating presynaptic glutamate autoreceptors and reducing the intensity and duration of cued reinstatement (35, 36). This possibility is directly supported by our finding that down-regulating ezrin to prevent the cued restoration of astroglia-Synapsin I proximity facilitates cue-induced heroin seeking. The regulation of synaptic glutamate release and spillover by astroglial processes is consistent with the fact that a 3–4-fold increase in selective postsynaptic astroglial coverage produces a 2–4-fold increase in the likelihood that glutamate escaping the synapse will activate presynaptic release-inhibiting autoreceptors (11, 37). Also, consistent with the idea that astroglial peripheral processes may provide a directional diffusion barrier, electron microscopy reveals that astroglial processes only partly contact synapses, with just 43% of the synaptic interface being contacted by astroglial membrane in rat hippocampus (38, 39), Thus, cue-induced restoration of astroglial surfaces near the synapse could target synaptic glutamate spillover towards presynaptic metabotropic glutamate autoreceptors and thereby reduce cue-induced glutamate release and reinstated heroin seeking. Indeed, preventing transient increase in astroglia-synapse proximity by ezrin knockdown prolonged the duration of reinstated heroin seeking, indicating that the plasticity may directly contribute to the gradual decrease (within-trial extinction) in unrewarded lever pressing that occurs over the 2 hr reinstatement session.

Conclusions and future directions

Our data show that rat NAcore astrocytes undergo transient re-association of astroglia-synapse proximity in response to heroin-associated cues, and that this plasticity negatively regulates cue-induced heroin seeking. A compensatory role for transient astroglial plasticity contrasts the transient postsynaptic potentiation (t-SP) produced in NAcore medium spiny neurons (MSNs) during cue-induced drug seeking (40, 41). The NAcore contains two subtypes of projection MSNs that selectively express either D1 or D2 dopamine receptors (42). Cued drug seeking is promoted by activating D1- or inhibiting D2-MSNs (43, 44), and postynaptic t-SP induced by drug cues occurs largely at D1-MSNs (45). Interestingly, individual astroglial Ca^{2+} flux selectively occurs in response to activity of either D1- or D2-MSNs (46). The cell specific associations by individual astroglia may contribute to the apparent subpopulations we observed in morphological characteristics, and it is interesting to speculate that the changes in astroglia-Synapsin I proximity may occur selectively around D1-MSNs that harbor cue-induced t-SP. The apparently opposing actions of cue-induced astroglial and postsynaptic plasticity highlights the importance of considering all four synaptic compartments (pre- and postsynapse, astroglial processes and extracellular matrix, (7, 31)) in order to understand how synapses are homeostatically balanced in contributing to behavior. Moreover, understanding tetrapartite synaptic homeostasis may be an important prerequisite towards developing interventions for behavioral pathologies such a drug relapse.

Supplementary Material

Refer to Web version on PubMed Central for supplementary material.

REFERENCES

1. Zhang Q, Pangrsic T, Kreft M, Krzan M, Li N, Sul JY, et al. (2004): Fusion-related release of glutamate from astrocytes. J Biol Chem. 279:12724–12733. [PubMed: 14722063]

2. Bernardinelli Y, Muller D, Nikonenko I (2014): Astrocyte-synapse structural plasticity. Neural Plast. 2014:232105. [PubMed: 24511394]

3. Khakh BS, Sofroniew MV (2015): Diversity of astrocyte functions and phenotypes in neural circuits. Nat Neurosci. 18:942–952. [PubMed: 26108722]

4. Perez-Alvarez A, Navarrete M, Covelo A, Martin ED, Araque A (2014): Structural and functional plasticity of astrocyte processes and dendritic spine interactions. J Neurosci. 34:12738–12744. [PubMed: 25232111]

5. Bernardinelli Y, Randall J, Janett E, Nikonenko I, Konig S, Jones EV, et al. (2014): Activity-dependent structural plasticity of perisynaptic astrocytic domains promotes excitatory synapse stability. Curr Biol. 24:1679–1688. [PubMed: 25042585]

6. Halassa MM, Fellin T, Takano H, Dong JH, Haydon PG (2007): Synaptic islands defined by the territory of a single astrocyte. J Neurosci. 27:6473–6477. [PubMed: 17567808]

7. Mulholland PJ, Chandler LJ, Kalivas PW (2016): Signals from the Fourth Dimension Regulate Drug Relapse. Trends Neurosci. 39:472–485. [PubMed: 27173064]

8. Scofield MD, Heinsbroek JA, Gipson CD, Kupchik YM, Spencer S, Smith AC, et al. (2016): The Nucleus Accumbens: Mechanisms of Addiction across Drug Classes Reflect the Importance of Glutamate Homeostasis. Pharmacol Rev. 68:816–871. [PubMed: 27363441]

9. Chaudhry FA, Lehre KP, van Lookeren Campagne M, Ottersen OP, Danbolt NC, Storm-Mathisen J (1995): Glutamate transporters in glial plasma membranes: highly differentiated localizations revealed by quantitative ultrastructural immunocytochemistry. Neuron. 15:711–720. [PubMed: 7546749]

10. Minelli A, Barbaresi P, Reimer RJ, Edwards RH, Conti F (2001): The glial glutamate transporter GLT-1 is localized both in the vicinity of and at distance from axon terminals in the rat cerebral cortex. Neuroscience. 108:51–59. [PubMed: 11738130]

11. Rusakov DA (2001): The role of perisynaptic glial sheaths in glutamate spillover and extracellular Ca(2+) depletion. Biophys J. 81:1947–1959. [PubMed: 11566769]

12. Pannasch U, Freche D, Dallerac G, Ghezali G, Escartin C, Ezan P, et al. (2014): Connexin 30 sets synaptic strength by controlling astroglial synapse invasion. Nat Neurosci. 17:549–558. [PubMed: 24584052]

13. Cheetham JJ, Hilfiker S, Benfenati F, Weber T, Greengard P, Czernik AJ (2001): Identification of synapsin I peptides that insert into lipid membranes. Biochem J. 354:57–66. [PubMed: 11171079]

14. Derouiche A, Frotscher M (2001): Peripheral astrocyte processes: monitoring by selective immunostaining for the actin-binding ERM proteins. Glia. 36:330–341. [PubMed: 11746770]

15. Lavialle M, Aumann G, Anlauf E, Prols F, Arpin M, Derouiche A (2011): Structural plasticity of perisynaptic astrocyte processes involves ezrin and metabotropic glutamate receptors. Proc Natl Acad Sci U S A. 108:12915–12919. [PubMed: 21753079]

16. Bushong EA, Martone ME, Jones YZ, Ellisman MH (2002): Protoplasmic astrocytes in CA1 stratum radiatum occupy separate anatomical domains. J Neurosci. 22:183–192. [PubMed: 11756501]

17. Reichenbach A, Derouiche A, Kirchhoff F (2010): Morphology and dynamics of perisynaptic glia. Brain Res Rev. 63:11–25. [PubMed: 20176054]

18. E.H.K. S (1990): The Intermediate Optical System of Laser-Scanning Confocal Microscopes Handbook of Biological Confocal Microscopy. Boston, MA: Springer.

19. Octeau JC, Chai H, Jiang R, Bonanno SL, Martin KC, Khakh BS (2018): An Optical Neuron-Astrocyte Proximity Assay at Synaptic Distance Scales. Neuron. 98:49–66 e49. [PubMed: 29621490]

20. Scofield MD, Li H, Siemsen BM, Healey KL, Tran PK, Woronoff N, et al. (2016): Cocaine Self-Administration and Extinction Leads to Reduced Glial Fibrillary Acidic Protein Expression and Morphometric Features of Astrocytes in the Nucleus Accumbens Core. Biol Psychiatry. 80:207–215. [PubMed: 26946381]

21. Kawaguchi K, Yoshida S, Hatano R, Asano S (2017): Pathophysiological Roles of Ezrin/Radixin/Moesin Proteins. Biol Pharm Bull. 40:381–390. [PubMed: 28381792]

22. Geiger KD, Stoldt P, Schlote W, Derouiche A (2000): Ezrin immunoreactivity is associated with increasing malignancy of astrocytic tumors but is absent in oligodendrogliomas. Am J Pathol. 157:1785–1793. [PubMed: 11106550]

23. Kirik OV, Korzhevskiy DE (2013): [Extraependymal ependymocytes in the rat brain]. Morfologiia. 143:71–73. [PubMed: 24020188]

24. Zhang Y, Chen K, Sloan SA, Bennett ML, Scholze AR, O'Keeffe S, et al. (2014): An RNA-sequencing transcriptome and splicing database of glia, neurons, and vascular cells of the cerebral cortex. J Neurosci. 34:11929–11947. [PubMed: 25186741]

25. Tsukita S, Yonemura S (1999): Cortical actin organization: lessons from ERM (ezrin/radixin/moesin) proteins. J Biol Chem. 274:34507–34510. [PubMed: 10574907]

26. Reissner KJ, Sartor GC, Vazey EM, Dunn TE, Aston-Jones G, Kalivas PW (2012): Use of vivo-morpholinos for control of protein expression in the adult rat brain. J Neurosci Methods. 203:354–360. [PubMed: 22027492]

27. Testen A, Sepulveda-Orengo MT, Gaines CH, Reissner KJ (2018): Region-Specific Reductions in Morphometric Properties and Synaptic Colocalization of Astrocytes Following Cocaine Self-Administration and Extinction. Front Cell Neurosci. 12:246. [PubMed: 30147645]

28. Robertson JM (2018): The Gliocentric Brain. Int J Mol Sci. 19.

29. Durkee CA, Araque A (2019): Diversity and Specificity of Astrocyte-neuron Communication. Neuroscience. 396:73–78. [PubMed: 30458223]

30. Allen NJ (2014): Astrocyte regulation of synaptic behavior. Annu Rev Cell Dev Biol. 30:439–463. [PubMed: 25288116]

31. Oliveira JF, Sardinha VM, Guerra-Gomes S, Araque A, Sousa N (2015): Do stars govern our actions? Astrocyte involvement in rodent behavior. Trends Neurosci. 38:535–549. [PubMed: 26316036]

32. Shen HW, Scofield MD, Boger H, Hensley M, Kalivas PW (2014): Synaptic glutamate spillover due to impaired glutamate uptake mediates heroin relapse. J Neurosci. 34:5649–5657. [PubMed: 24741055]

33. Henneberger CB L; Panatier A; Reynolds JP; Medvedev NI; Minge D; Herde MK; Anders S; Kraev I; Zheng K; Jensen T; Sanchez-Romero I; Janovjak H; Ottersen OP; Nagelhus EA; Oliet SHR; Stewart MG; Nagerl UV; Rusakov DA (2018): Astroglia withdraw from potentiated synapses boosting inter-synaptic cross-talk. bioRxiv.

34. Danbolt NC (2001): Glutamate uptake. Prog Neurobiol. 65:1–105. [PubMed: 11369436]

35. Dietrich D, Kral T, Clusmann H, Friedl M, Schramm J (2002): Presynaptic group II metabotropic glutamate receptors reduce stimulated and spontaneous transmitter release in human dentate gyrus. Neuropharmacology. 42:297–305. [PubMed: 11897108]

36. Scofield MD, Boger HA, Smith RJ, Li H, Haydon PG, Kalivas PW (2015): Gq-DREADD Selectively Initiates Glial Glutamate Release and Inhibits Cue-induced Cocaine Seeking. Biol Psychiatry. 78:441–451. [PubMed: 25861696]

37. Lehre KP, Rusakov DA (2002): Asymmetry of glia near central synapses favors presynaptically directed glutamate escape. Biophys J. 83:125–134. [PubMed: 12080105]

38. Ventura R, Harris KM (1999): Three-dimensional relationships between hippocampal synapses and astrocytes. J Neurosci. 19:6897–6906. [PubMed: 10436047]

39. Witcher MR, Kirov SA, Harris KM (2007): Plasticity of perisynaptic astroglia during synaptogenesis in the mature rat hippocampus. Glia. 55:13–23. [PubMed: 17001633]

40. Gipson CD, Kupchik YM, Shen H, Reissner KJ, Thomas CA, Kalivas PW (2013): Relapse induced by cues predicting cocaine depends on rapid, transient synaptic potentiation. Neuron. 77:867–872. [PubMed: 23473317]

41. Gipson CD, Kupchik YM, Kalivas PW (2014): Rapid, transient synaptic plasticity in addiction. Neuropharmacology. 76 Pt B:276–286. [PubMed: 23639436]

42. Soares-Cunha C, Coimbra B, Sousa N, Rodrigues AJ (2016): Reappraising striatal D1- and D2-neurons in reward and aversion. Neurosci Biobehav Rev. 68:370–386. [PubMed: 27235078]

43. Lobo MK, Nestler EJ (2011): The striatal balancing act in drug addiction: distinct roles of direct and indirect pathway medium spiny neurons. Front Neuroanat. 5:41. [PubMed: 21811439]

44. Heinsbroek JA, Neuhofer DN, Griffin WC 3rd, Siegel GS, Bobadilla AC, Kupchik YM, et al. (2017): Loss of Plasticity in the D2-Accumbens Pallidal Pathway Promotes Cocaine Seeking. J Neurosci. 37:757–767. [PubMed: 28123013]

45. Bobadilla AC, Heinsbroek JA, Gipson CD, Griffin WC, Fowler CD, Kenny PJ, et al. (2017): Corticostriatal plasticity, neuronal ensembles, and regulation of drug-seeking behavior. Prog Brain Res. 235:93–112. [PubMed: 29054293]

46. Martin R, Bajo-Graneras R, Moratalla R, Perea G, Araque A (2015): Circuit-specific signaling in astrocyte-neuron networks in basal ganglia pathways. Science. 349:730–734. [PubMed: 26273054]
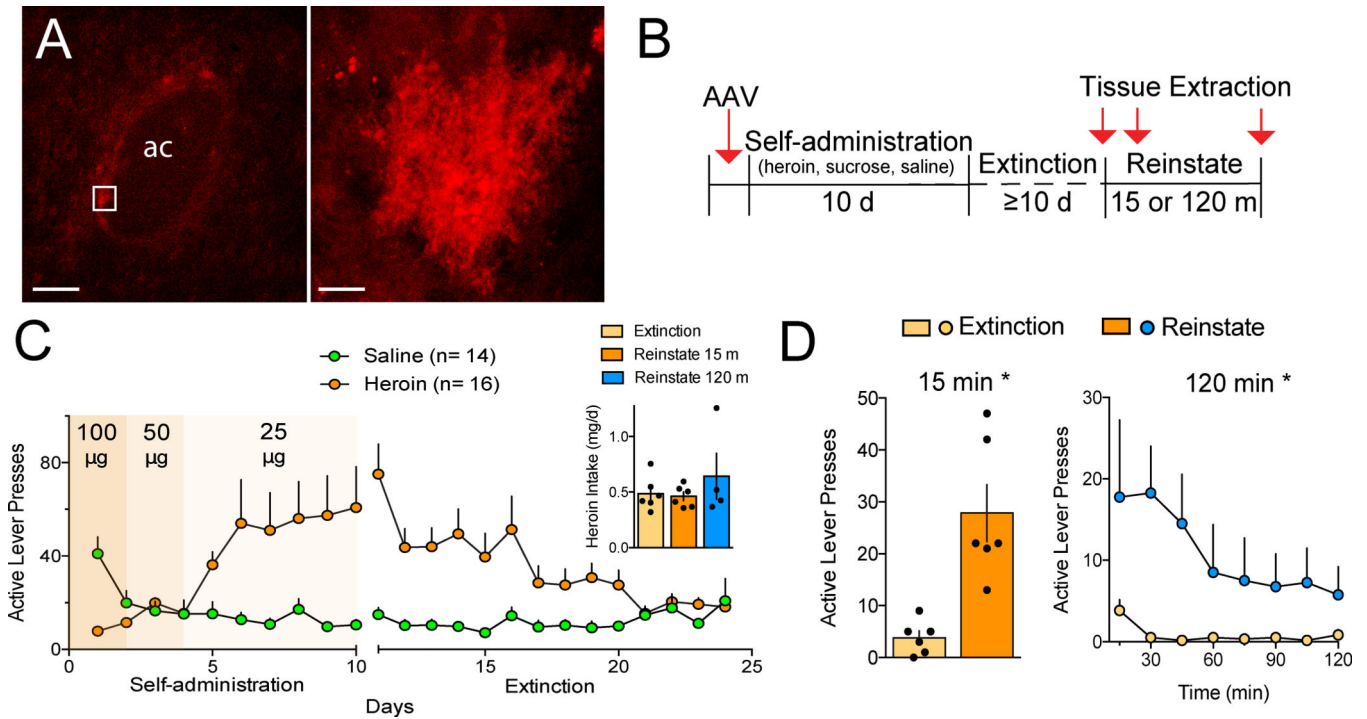
Figure 1.

Heroin self-administration and cue-induced heroin seeking. (**A**) Representative transfection of astroglia in the NAcore with an AAV driving membrane-bound mCherry under the GFAP promoter. Low magnification (left) shows multiple filled astroglia adjacent to the anterior commissure (ac; bar=150 μm), and high magnification (right) shows a single astrocyte (bar=10 μm). (**B**) Outline of the protocol used throughout the manuscript. (**C**) Active lever pressing during heroin self-administration and extinction training (see Supplemental Figure S2 for inactive lever pressing). Inset shows that the treatment groups infused the same total amount of heroin (1-way ANOVA, $F_{(2,13)}$= 0.84, p= 0.455). (**D**) 15 or 120 min of cue-induced reinstatement elevated active lever pressing compared to the first 15 min of the final extinction trial (15 min-paired Student's $t_{(5)}$= 3.77, p= 0.013; 120 min- 2-way repeated measures ANOVA treatment $F_{(1,3)}$= 10.06, p= 0.050). Data shown as mean±sem.
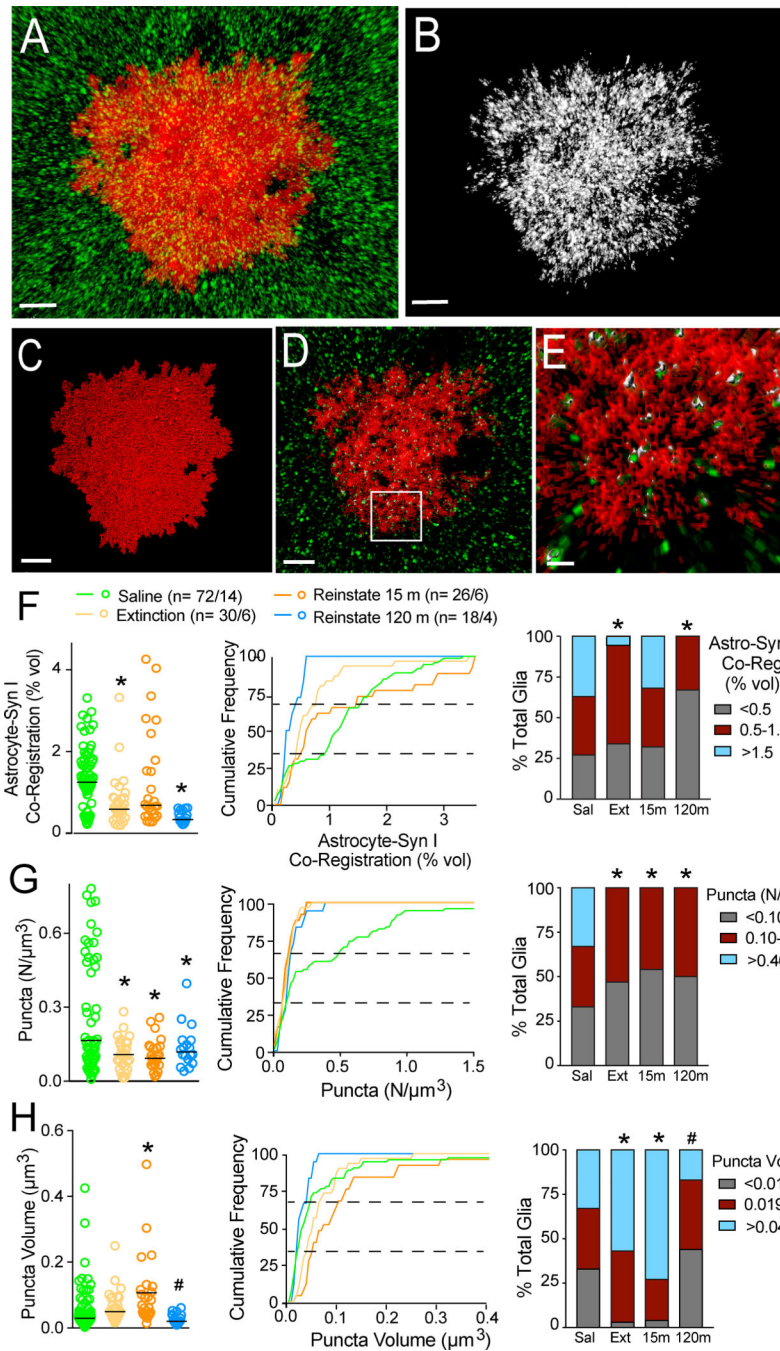
Figure 2.

Co-registration of the astroglial membrane with Synapsin I undergoes transient plasticity during cued heroin seeking. (**A**) Representative confocal image of an astrocyte (red) that was counter-stained for immunoreactive Synapsin I (green). (**B**) Right panel shows digitally isolated Synapsin I puncta that co-registered with the astroglial membrane (within 250 nm). (**C**) Digital render of the astrocyte in **A**. (**D**) A single plane from the middle of the Z-axis in **A**. (**E**) Co-registered astroglial membrane (red) and Synapsin I (green) from the box in **D**. Astroglial membranes within 250 nm of Synapsin I puncta are colored white versus green

puncta not within the 250 nm limit of resolution. (**F**) Synaptic proximity of the astroglial membrane was constitutively reduced after extinguished withdrawal and transiently increased during 15 min of cued heroin seeking (left panel raw data Kruskal-Wallis= 18.8 p< 0.001; middle panel shows cumulative frequency plots; right panel shows subpopulations: $Chi^2_{(6)}$= 23.78, p< 0.001). (**G**) The number of co-registered puncta was reduced after heroin self-administration (left panel raw data Kruskal-Wallis= 16.42 p= 0.001; middle panel show frequency plots; right panel shows subpopulations: $Chi^2_{(6)}$= 29.86, p< 0.001). (**H**) Average volume of co-localized puncta was increased after 15 min of reinstated heroin seeking (left panel raw data Kruskal-Wallis= 25.8 p< 0.001; middle panel shows frequency plots; right panel shows subpopulations: $Chi^2_{(6)}$= 27.51, p< 0.001). *p< 0.05, compared to saline using a Dunn's post hoc (left panel) or multiple Chi^2 tests with a Bonferroni adjustment for multiple comparisons (right panel), #p< 0.05, compared to reinstate 15 min. (**A-D**) bar=10 μm, (**E**) bar=2 μm. (**F-H**) left panel, bar = median.
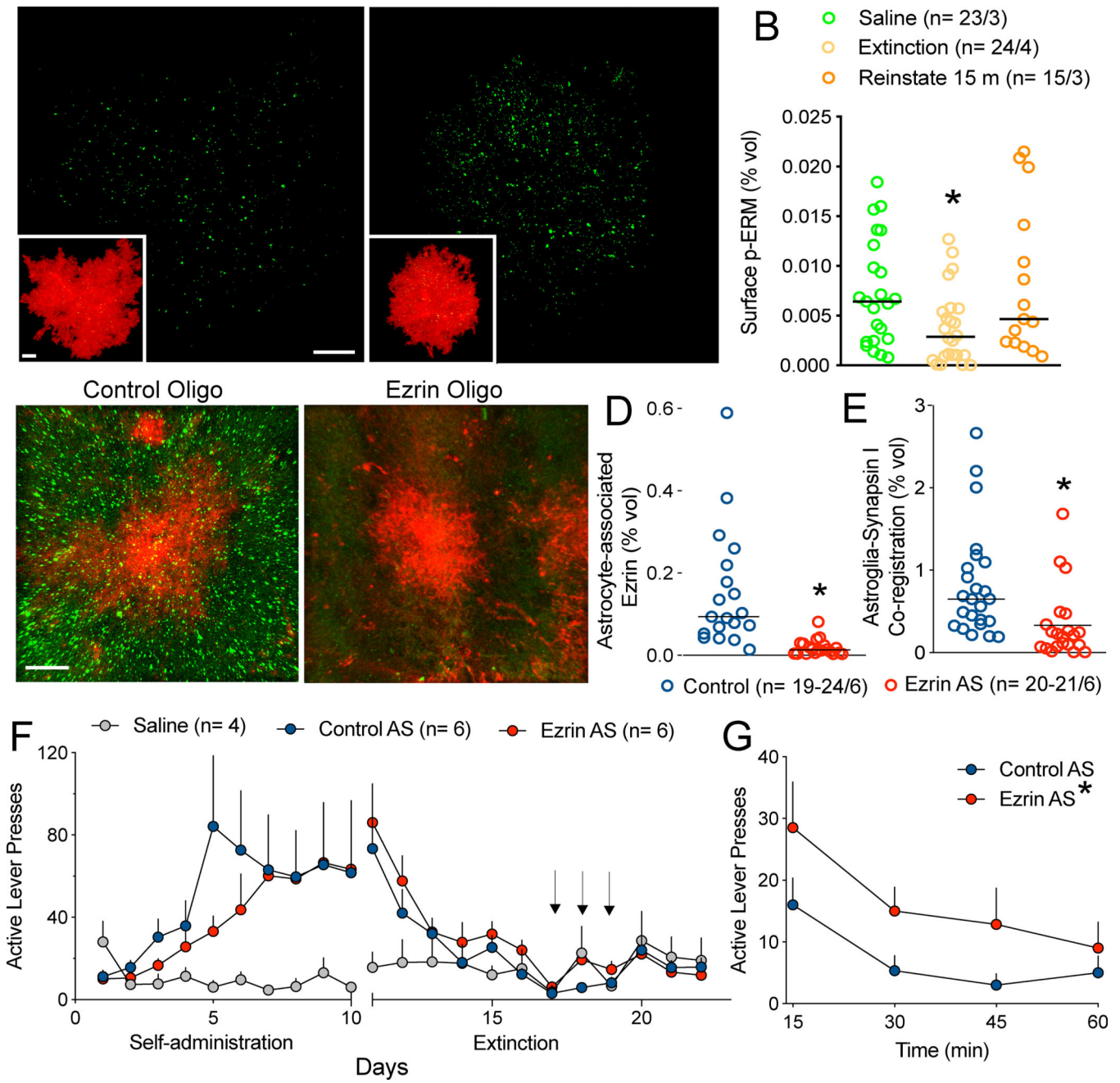
Figure 3.
Ezrin knockdown prevents transient astroglial plasticity and promotes cue-induced heroin seeking. (**A**-**B**) p-ERM immunoreactivity was examined in tissue extracted from animals following extinction or after 15-min of reinstatement with heroin cues (see Supplemental Figure S6 for inset magnification). (**B**) Heroin cues elicited a significant elevation in p-ERM levels compared to those observed in extinguished animals (Kruskal-Wallis= 7.483 p= 0.0237) and an ezrin-targeted antisense oligo was developed to knock down ezrin expression (**C**-**D**). Relative to a control oligo (**C**), the ezrin-targeted morpholino oligo produced 86% ezrin knockdown (reduction in green fluorescence) near the injection tract (**D**; Mann-

Whitney t-test, p= 0.0007). The ezrin-targeted oligo produced a profound reduction in synaptic association of astroglial membrane (**E**, Mann-Whitney t-test, p= 0.0003). (**F**) Next, rats were trained to self-administer heroin for 10d before undergoing extinction training. On d7 of extinction, rats received bilateral infusions of the ezrin-targeted antisense oligomer or a control oligo for three consecutive days in the NAcore (arrows). Animals from both groups were reinstated using cues and animals that underwent ezrin knockdown exhibited enhanced and prolonged reinstatement behavior compared to controls (**G**, 2-way ANOVA, $F_{(1, 40)}$= 8.193, p= 0.0067, effect of treatment). In (**B, D-E**), n is shown in legends as cells/animals. (**G**) 1-way ANOVA, $F_{(2,13)}$= 0.84, p= 0.455. In (**E, J**), data shown as mean±sem; in (**D, H, I**) data shown as median. Bar= 10 μm (**A**), 10 μm (inset), 20 μm (**C**).